Chemistry of Hydrogen-Octasilsesquioxane: Preparation and Characterization of Octasilsesquioxane-Containing Polymers

Norbert Auner,[†] Jan W. Bats,[†] Dimitris E. Katsoulis,[‡] Michitaka Suto,[§] Ronald E. Tecklenburg,[‡] and Gregg A. Zank*[,§]

Inst. fur Anorg. Chemie, Johann Wolfgang Goethe University, Marie-Curie-Str. 11, D - 60439 Frankfurt/Main, Mertonviertel, Oberursel, Dow Corning Corporation, Midland, Michigan 48686-0995, and Dow Corning Asia, Ltd., 603 Kishi, Yamakita, Kanagawa 258-0112, Japan

Received April 18, 2000. Revised Manuscript Received August 30, 2000

Over the past five years, there have been a number of studies that have concerned themselves with controlling the structure of inorganic networks. Many of these studies have been undertaken due to the need for more advanced or structurally ordered materials in a variety of electrical and optical applications. One of the approaches to create materials that are structurally ordered has been to assemble the higher molecular weight polymers and materials not from monomeric precursors but from partially assembled oligomeric structural building blocks. In the silicone materials area, the well-known completely condensed cages T_n or Q_n^{n-} offer convenient higher order building blocks for larger structural assemblies. In most cases materials made by employing these cages as the building blocks have afforded gels or insoluble network materials due to the high degree of functionality (typically *n*) present in these building blocks. In this paper, we report the preparation of soluble resins that are $^{H}T_8$ cages linked together with divinyl species as links made by hydrosilation chemistry and their characterization as it relates to previously reported studies. We have employed a range of linking groups (L) from organics (divinyl benzene) and α−Ω functional siloxanes (from a degree of polymerization, DP, of 2−12). Interestingly, we have also found it possible to make soluble network materials even when employing two linking groups (L) per cage. We have combined the characterization of the high-molecular-weight polymers with detailed characterization of small molecules made by these same hydrosilation reactions to provide insights into some relatively simple model Si−resin systems. The characterization of these relatively simple systems helps provide insights into the structure ↔ property relationships of silicone materials in general.

I. Introduction

Silsesquioxanes or three-dimensional silicone resins, typically prepared from the hydrolytic condensation of $RSiX_3$ (X = Cl or OMe or OEt), have a long history and continue to be materials of interest. The application areas for silicone resins range from coatings to protect from heat or abrasion, electrically insulating coatings, processing aids or modifiers for organic polymers, interlayer dielectrics, and precursors to crystalline silicon carbide ceramics. While the commercial successes have been numerous for these silicone resins, comparatively little is known about the structure of these materials. This lack of knowledge leaves a substantial void in trying to complete process ↔ structure ↔ property relationship understandings for silicone resins. The characterization of these largely amorphous materials is not a trivial task even when employing the most advanced analytical techniques that are available today.

Adding to the difficulty of structure characterization of silicone resins is the fact that there are relatively few highly branched polymeric silicone materials where at least a portion of the structure is well-known. Completely condensed silsesquioxane and silicate cages represent an appealing molecular "model" for silicone resins. However, despite a number of publications on the synthesis and reactivity of unique silsesquioxane and silicate cages it is not clear if they are a unique class of materials themselves or are more appropriately viewed as building blocks of the wider class of silicone resins.[1] We report here the preparation of soluble resins that are comprised of cages linked together ($^{H}T_8$ and divinyl species as links made by hydrosilation chemistry) as well as their characterization that demonstrates that the cages are intact in the polymeric material.

There are a number of gels or insoluble network materials that are known to contain complete cages as an integral part of the network.[2] Specifically, two research groups lead by Höebbel and Hasegawa have

* g.a.zank@dowcorning.com.
[†] Johann Wolfgang Goethe University.
[‡] Dow Corning Corporation.
[§] Dow Corning Asia, Ltd.

(1) Brevett, C. S.; Cagle, P. C.; Klemperer, W. G.; Ruben, G. C. *J. Inorg. Organometal. Polym.* **1991**, *1* (3), 335−342.
(2) Harrison, P. G. *J. Organometal. Chem.* **1997**, *542*, 141−83.

10.1021/cm000325e CCC: $19.00 © 2000 American Chemical Society
Published on Web 10/14/2000

extensively studied materials that contain complete cages as part of the network. The route studied by Höebbel involves making $^{R}T_8$ cages [R = H or Vi, T = $RSiO_{3/2}$] or $^{R}M_8Q_8$ [R = H or Vi, M = $R_3SiO_{1/2}$; Q = $SiO_{4/2}$] and linking them together through hydrosilation.[3] This chemistry has also employed the use of additional functional silicones to act as bridges between the cages.[4]

From the characterization that has been carried out on these network materials, typically above 60% and more commonly greater than 80% of the functionality, Si−H and Si−Vi are consumed to make silethylene linkages in the hydrosilation. With this type of conversion efficiency of the organic functionality, it is not surprising that none of the materials are soluble since nearly all of the precursors are octafunctional. While most of these three-dimensional network materials have not received a lot of characterization, there has been some discussion concerning their porosity. In general, few of these materials show substantial porosities after gelation. In the literature, there are many inconsistencies regarding these materials which can be viewed as "isocompositional" but have shown different porosities, depending on the specifics of the synthesis route, and hence are not isostructural.[3−7]

In an effort to consistently compare one set of materials to another, Laine et al. have published a complete study which describes both the synthesis and characterization of gels made from reactions combining the $^{H}M_8Q_8$, $^{Vi}M_8Q_8$, $^{H}T_8$, and $^{Vi}T_8$.[6] In this study, the gelation was conducted at room temperature over time frames up to 9 h in dilute toluene solutions. With this synthetic method, all of the materials were found to be a combination of micro- and mesoporous with specific surface areas between 380 and 530 m^2/g. In this work, the researchers begun to correlate the pore sizes seen in the materials to the distances seen from the cage and the linking group distances in the idealized structures. Intercube pore size was dominated by the length of the siloxane spacer and that dimension was preserved in the actual material microstructure.

Employing this approach of hydrosilating one cage to another**,** one soluble material has been reported by Höebbel. It was made employing the ratio of $^{Vi}M_8Q_8$/$^{H}M_8Q_8$ of 1/0.25. By changing the stoichiometry of the reaction in this way, the researchers effectively limited the extent of cross-linking as only two of the vinyl groups on the $^{Vi}M_8Q_8$ could on average react.[8] The only characterization of this soluble material given was a solution ^{29}Si NMR spectrum, since the focus of the work was to make insoluble materials.

Hasegawa employed a similar approach to linking Q_8 cages together, which eliminated the silethylene linkage afforded by the hydrosilation and made the linkage more inorganic in nature.[7] The general approach employs the reaction of solutions of the octa-anion Q_8^{8-} with 4 equiv of Me_2SiCl_2. While this provided an even shorter linkage and presumably one that had less flexibility, the resulting material gel was not very porous and had a low surface area of about 30 m^2/g. As was discussed above, the low specific surface areas are not entirely due to the type of linking group employed but rather are due to a number of factors, most notably the synthetic procedures employed, as was demonstrated by the work of Laine et al.[6]

From the literature, one can find four approaches that have been employed to incorporate T_8-type cages in the backbone of soluble polymers. The first approach involved the use of partial cages and has been championed by Lichtenhan.[9] In this chemistry, the synthesis of a difunctional cage $(CySiO_{1.5})_6(CySiO(OH))_2$, [Cy = cyclohexyl] a so-called $^{Cy}T_6{}^{Cy}T^2{}_2$, was the key building block. This partial cage was then reacted with difunctional linear silicones to make "bead-type" polymers that are claimed to have perfectly alternating linear bead arrangement (see eq 1).

These researchers also investigated the preparation of organically modified materials with pendant and bead-type architectures.[10] The bead-type architecture is the most relevant one to the work described herein. As can be seen from their single crystal X-ray diffraction work the partial cage that has led to the bead-type polymers bears little resemblance to its completely condensed T_8 cage precursor, unlike the depiction in the drawing of eq 1.[11]

A second approach to making soluble polymers with T_8-type cages in the backbone involves the derivatization of the $^{H}T_8$ cage with organic groups that can later be polymerized. Typically, this derivatization was carried out to prepare $^{R}T_8$-type of materials as has been demonstrated by Bassindale.[12] When the organic moiety R contains a latent (typically organic) functionality, the resulting $^{R}T_8$ could be polymerized. Given the high degree of functionality, this most commonly led to formation of an insoluble material, as was the case with

(3) Hoebbel, D.; Enders, K.; Reinert, T.; Pitsch, I. *J. of Non-Cryst. Solids* **1994**, *176*, 179−88.

(4) (a) Hoebbel, D.; Enders, K.; Reinert, T.; Schmidt, H. *New Routes to Silicic Acid Containing Inorganic−Organic Hybrid Precursors and Polymers*, 6th ed.; Hoebbel, D., Enders, K., Reinert, T., Schmidt, H., Eds.; Materials Research Society: San Francisco, CA, 1994; Vol. 346, pp 863−74.

(5) Harrison, P. G.; Kannengiesser, R. *J. Chem. Soc., Chem. Commun*. **1996**, 415−16.

(6) Zhang, C.; Babonneau, F.; Bonhomme, C.; Laine, R. M.; Soles, C. L.; Hristov, H. A.; Yee, A. F. *J. Am. Chem. Soc.* **1998**, *120*, 8380−91.

(7) (a) Hasegawa, I.; Ishida, M.; Motojima, S.; Satokawa. *Organic-Silica Hybrid Materials Consisting of the Double Four-Ring Structure as a Building Block*, 6th ed.; Hasegawa, I., Ishida, M., Motojima, S., Satokawa, Eds.; Materials Research Society: San Francisco, CA, 1994; Vol. 346, pp 163−67. (b) Hasegawa, I. *J. Sol−Gel Sci. Technol.* **1995**, *5*, 93−100.

(8) Hoebbel, D.; Pitsch, I.; Heldemann, D.; Jancke, H.; Hiller, W. *Z. Anorg. Allg. Chem*. **1990**, *583*, 133−44.

(9) (a) Lichtenhan, J. D.; Vu, N. Q.; Carter, J. A.; Gilman, J. W.; Feher, F. J. *Macromolecules* **1993**, *26*, 2141−2. (b) Mantz, R. A.; Jones, P. F.; Chaffee, K. P.; Lichtenhan, J. D.; Gilman, J. W.; Ismail, I. M. K.; Brumeister, M. J. *Chem. Mater.* **1996**, *8*, 1250−9. (c) Lichtenhan, J. D.; Haddad, T. S.; Schwab, J. J.; Carr, M. J.; Chaffee, K. P.; Mather, P. T. *Polym. Prepr.* **1998**, *39*, 489−90.

(10) (a) Shockey, E.; Lichtenhan, J. D. *Polym. Prepr.* **1995**, *36*, 138−9. (b) Haddad, T. S.; Choe, E.; Lichtenhan, J. D. *Hybrid Styryl-Based Polyhedral Oligomeric Silsesquioxanes (POSS) Polymers*; Haddad, T. S., Choe, E., Lichtenhan, J. D., Eds.; Materials Research Society: San Francisco, CA, 1996; Vol. 435, pp 25−32. (c) Lichtenhan, J. D.; Noel, C. J.; Bolf, A. G.; Ruth, P. N. *Thermoplastic Hybrid Materials: Polyhedral Oligomeric Silsesquioxane (POSS) Reagents, Linear Polymers and Blends*; Lichtenhan, J. D., Noel, C. J., Bolf, A. G., Ruth, P. N., Eds.; Materials Research Society: San Francisco, CA, 1996; Vol. 435, pp 3−11. (d) Romo-Urbie, A.; Mather, P. T.; Haddad, T. S.; Lichtenhan, J. D. *J. Polym. Sci., Part B: Polym. Phys.* **1998**, *36*, 1857−72.

(11) Lichtenhan, J. D.; Haddad, T. S.; Schwab, J. L.; Carr, M. J.; Chaffee, K. P.; Mather, P. T. *Polym. Prepr.* **1998**, *39*, 489−90.

(12) (a) Bassindale, A. R.; Gentle, T. E. *J. Mater. Chem.* **1993**, *3*, 1319−25. (b) Gentle, T. E.; Bassindale, A. R. *J. Inorg. Organomet. Polym*. **1995**, *5*, 281−94.

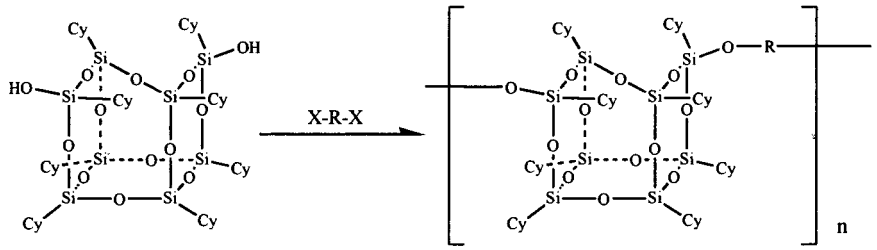

(1)

R = Me_2Si, $(Me_2SiO)_n$, RR'Si, silethylene and silphenylene materials

methacrylate and epoxy-functional $^{R}T_8$ molecules.[13] There are two examples however of making soluble polymeric materials from the thermal polymerization of octafunctional $^{R}T_8$ where R was epoxyhexene or propyloxyvinyl ether.[14] In this work, the authors attributed the formation of soluble materials to the fact that a relatively high number of these reactions took place by an intramolecular process, thereby lowering the overall cross-link density of the material despite the extent of the reaction being about 90%.

Rebrov et al. described potentially a third approach to make soluble polymers with T_8-type cages in the backbone involving the formation of pure "parafunctional" $^{Me}T_6{}^{Vi}T_2$ cages (eq 2) and the subsequent polymerization by hydrosilation with dihydrido-functional siloxanes.[15]

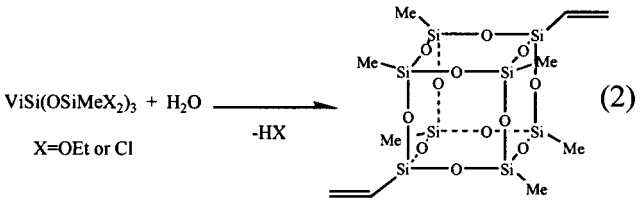

(2)

The authors provided very few experimental details for their complicated synthesis, and the resulted polymers were not well-characterized beyond GPC DSC and TGA weight loss. More recently a pure "para-inorganofunctional" cage has been reported from the reaction of $^{H}T_8$ and acetone in the presence of water and pyridine with dicobalt octacarbonyl as a catalyst.[16] This cage obtained in 35% yield is shown in Structure 1.

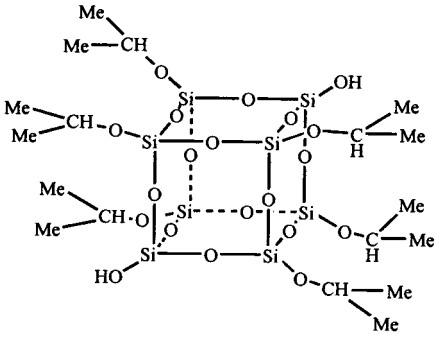

structure 1

The fourth approach to making soluble polymers with T_8-type cages in the backbone involved the hydrosilation of $^{H}T_8$ to organic acetylenes or sterically hindered diynes, in particular, 1,3-phenylethynylbenzene, to produce polymers that contained both latent Si−H and C=C functionality (eqs 3 and 4).[17]

Monomeric materials were prepared employing this approach. The chemistry described in eq 3 was carried out for only 10 min, and the products were isolated by preparative GPC. The reaction described in eq 4 was carried out over 3 h and afforded polymeric materials in 60% yield after isolation again by preparative GPC. These products had molecular weights that were dependent on the diyne to $^{H}T_8$ material stoichiometry (21 000 for 1.2:1.0 and 87 000 for 1.55:1.0). Both material stoichiometries exhibited high thermal stabilities, showing only 5% weight loss upon heating to ∼1000 °C in nitrogen. The same chemistry of $^{H}T_8$ and diynes can be used to make other polymeric materials as depicted in eq 4. Two examples have been demonstrated where the $-C_6H_4-$ was changed to Me_2Si or ferrocene. These materials were obtained at low-to-moderate yields and showed reasonably high molecular weights [M_n of about 10^4], good thermal stability in air, and excellent ceramic yields under nitrogen as measured by TGA. Due to the high functionality in the organic moiety and the octafunctionality in the cage, it is very likely that more than just the desired two hydrosilations took place, thereby reducing the overall yield of the soluble material. GPC separation/fractionation was used to isolate Pt-free products and terminate the reaction. The facile chemistry of bishydrosilation is shown in eq 5.

The bishydrosilation product of phenyl acetylene and $^{H}T_8$ was obtained after stirring the reaction mixture at ambient temperatures for 3 days.[18] This polymeric material (yield 40%) had molecular weights of M_n = 11 000 and M_w = 15 000. The extent of hydrosilation was effectively controlled through the reaction time and by isolation of Pt-free products by preparative GPC.

According to these researchers, the hydrosilation of diynes with $^{H}T_8$ was carried out to produce heat resistant or porous materials. When considering dienes,

(13) (a) Sellinger, A.; Laine, R. M. *Macromolecules* **1993**, *29*, 2327−30. (b) Zhang, C.; Laine, R. M. *J. Organomet. Chem.* **1996**, *521*, 199−201.

(14) Crivello, J. V.; Malik, R. *J. Polym. Sci., Part A: Polym. Chem.* **1997**, *35*, 407−25.

(15) (a) Rebrov, E. A.; Tebeneva, N. A.; Mouzafarov, A. M.; Ovchinnikov, Y. E.; Struchkov, Y. T.; Strelkova, T. V. *Russin Chem. Bull. (Engl. Trans.)* **1995**, *44*, 1286−92. (b) Tebeneva, N. G.; Rebrov, E. A.; Muzafarov, A. M. *Polym. Prepr.* **1998**, *39*, 503−4.

(16) Said, M. A.; Roesky, H. W.; Rennekamp, C.; Andruh, M.; Schmidt, H.-G.; Noltemeyer, M. *Angew. Chem., Int. Ed. Engl.* **1999**, *38*, 661−4.

(17) Kobayashi, T.; Hayashi, T.; Tanaka, M. *Chem. Lett.* **1998**, 763−4.

(18) Kobayashi, T.; Hayashi, T.; Tanaka, M. *New Silsesquioxane Containing Polymer: Its Preparation Method and Thermal Resistant Material*; Kobayashi, T., Hayashi, T., Tanaka, M., Eds.: Japan, 1997.

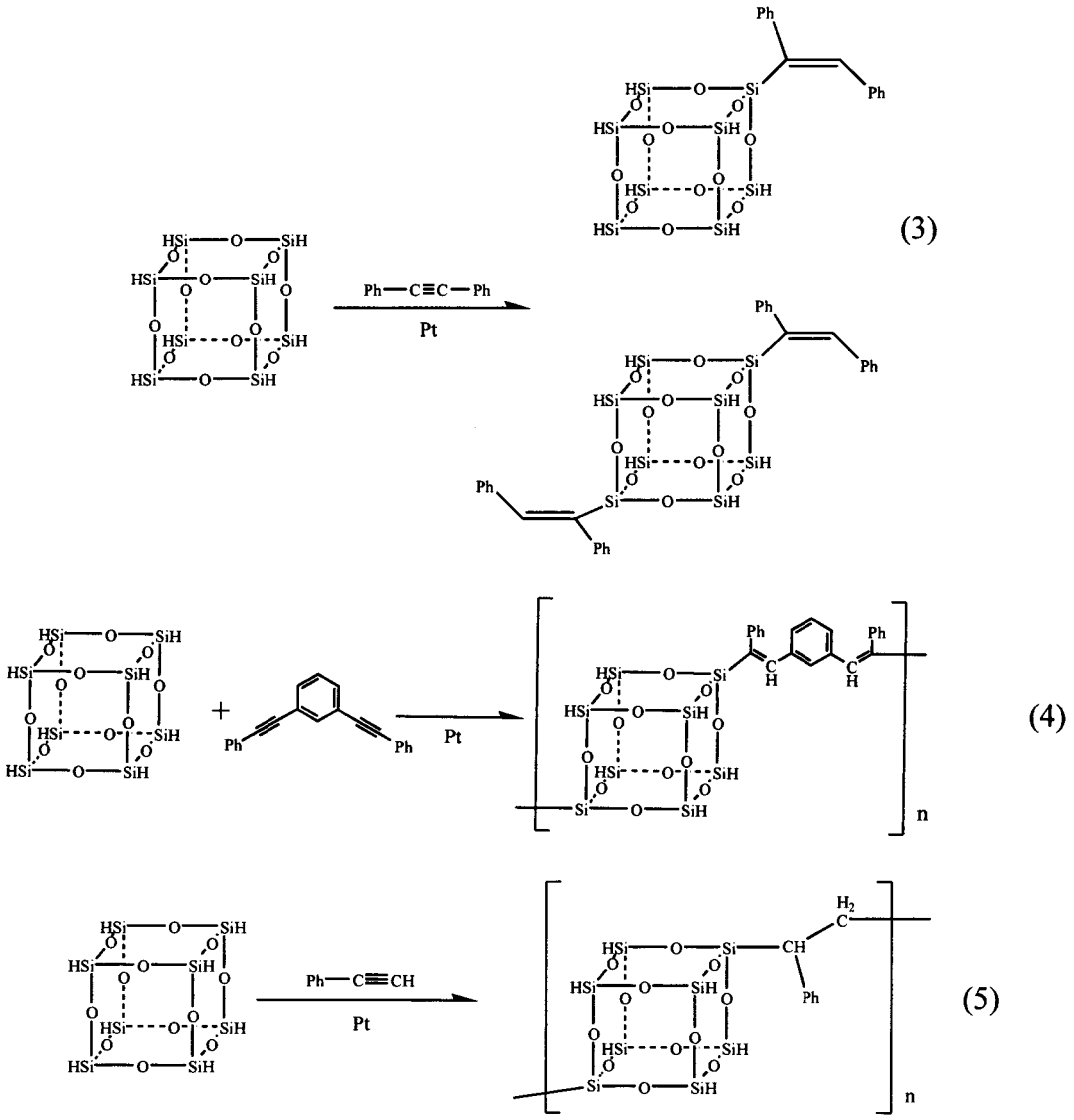

these researchers cite prior publications that show "Hydrolysis polymerization and hydrosila-polymerization of substituted T_8 species are reported to give heat-resistant and/or porous materials." However, these products were usually gels and not soluble in organic solvents.[17] The chemistry we describe here shows that with careful dilution and control over the reaction stoichiometry we can control the hydrosilation of $^{H}T_8$ with both organic and inorganic dienes, to form soluble resins in essentially quantitative yields.

II. Experimental Section

A. Materials. The platinum catalyst, a dimethylvinyldisiloxane complex in toluene, was obtained as a Dow Corning intermediate. $^{H}T_8$ was prepared according to the method of Frye and Collins.[19] All other materials were purchased and used without further purification.

B. General Polymer Synthesis. All of these reactions were carried out as a homogeneous toluene solution, with a $^{H}T_8$ concentration of ~0.05 M under N_2. The platinum catalyst employed was a dimethylvinyldisiloxane complex in toluene. The platinum concentration of this solution was 200 ppm, and the amount used in the polymer synthesis was ~250 μL/g of $^{H}T_8$. The following is a specific example which depicts the procedure used to make the polymers summarized in Table 1.Into a N_2-purged, 1 L three-necked reaction flask equipped with a magnetic stirring bar and fitted with an air-cooled condenser was placed 13.5 g (0.032 mol) of $^{H}T_8$ and 5.95 g (0.032 mol) of $(ViMe_2Si)_2O$ which was dissolved in 700 mL of toluene that was distilled from sodium under nitrogen. To this was added the platinum catalyst (5 mL) with stirring. After the addition of the reactants, solvent, and catalyst, the reaction was maintained at 60 °C for 20 h, and the solution was then cooled, filtered, and evaporated to dryness with a rotary evaporator, followed by drying at ambient temperatures under a dynamic vacuum. The polymer was separated from the small amount of excess $^{H}T_8$ by extraction with 75 mL of MIBK and filtration to remove the sparingly soluble $^{H}T_8$ (1.7 g). The MIBK was then removed from the filtrate in vacuo, and the solid polymer was dried under a dynamic vacuum for 3 h at 40 °C. Yield: 16.25 g or 91.3% of theoretical.

C. Preparation of Model Compounds. *Reaction of $(ViMe_2Si)_2O$ with $^{H}T_8$.* Into a 5 L, three-necked reaction flask under N_2 with a magnetic stirring bar and fitted with an air-cooled condenser was placed 8.00 g (0.018 86 mol) of $^{H}T_8$ which was dissolved in 2000 mL of toluene that was distilled over sodium under nitrogen. A platinum catalyst was added to this solution (50 μL) delivered as a complex with $ViMe_2SiOSiMe_2$-Vi in a 200 ppm toluene solution. To this was added 0.877 g (0.0047 mol) of $(ViMe_2Si)_2O$ as a toluene 300 mL solution over a 3 h period at 60 °C. The resulting reaction was maintained at 60 °C for 3, and the solution was then cooled, filtered, and

(19) Frye, C. L.; Collins, W. T. *J. Am. Chem. Soc.* **1970**, *92*, 5586–8.

Table 1. Polymer Compositions and Yields

link	$^{H}T_8$:link	isolated yield %
$^{Vi}M^{Vi}M$	1:1	91.3
$^{Vi}M^{Vi}M$	1:1.5	86.4
$^{Vi}M^{Vi}M$	1:2	95.7
$^{Vi}MD_5ViM$	1:1	84.2
$^{Vi}MD_8ViM$	1:1	92.4
$^{Vi}MD_8ViM$	1:2	86.4
$(Ph_2ViSi)_2O$	1:1	93.5
dvb[a]	1:1	92.4

[a] dvb is a mixture of isomers of divinylbenzene.

Table 2. GPC Characterization of the Materials

linking group Vi−L−Vi	link:cage	M_n	M_w	Pd
$-Me_2SiOSiMe_2-$	1:1	3 088	79 390	25
		5 570[a]	45 300[a]	7.9[a]
	1.5:1	3 610	93 400	26
		4 770[a]	116 300[a]	24.4[a]
	2:1	6 355	331 400	52
		36 400[a]	677 500[a]	18.6[a]
$-Ph_2SiOSiPh_2-$	1:1	1 459	2 655	1.8
$-(Me_2SiO)_7-$	1:1	4 112	823 000	200
$-(Me_2SiO)_{10}-$	1:1	3 250	7 785	2.4
	2:1	18 720	1 092 700	99
$-(C_6H_4)-$	1:1	9 592	46 120	4.8
	2:1	12 246	1 066 750	87

[a] Employed GPC[3] with universal calibration method.

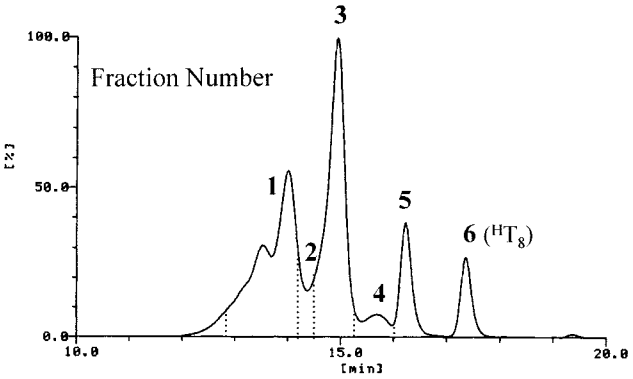

Figure 1. Analytical GPC trace of reaction product forms of $(ViMe_2Si)_2O$ and $^{H}T_8$ at a stoichiometry of 0.25:1.

evaporated to dryness with a rotary evaporator, followed by drying at ambient temperatures under a dynamic vacuum. The hydrosilated reaction product was separated from the majority of excess $^{H}T_8$ by extraction of the residue with 25 mL of MIBK and filtering to remove the sparingly soluble $^{H}T_8$ (5.10 g). The MIBK was then removed from the filtrate in vacuo, and the residue was dissolved in toluene at 3 wt % solids. The individual components in the toluene solution were then separated into six fractions by preparatory gel permeation chromatography. The individual fractions were then vacuum stripped to dryness using a rotary evaporator, and the white solid residues were removed from the flask.

D. Growth of Single Crystals. Into a 5 mL vial was dissolved 20 mg of the material designated as fraction 5 from the preparative GPC experiment described in section C above and 4 mL of toluene. The toluene solution was then allowed to slowly evaporate, thereby affording single crystals suitable for single-crystal diffraction studies. A ruler-shaped crystal of the approximate dimensions 0.6 × 0.34 × 0.07 mm was chosen for the crystal structure analysis.

E. Characterization. Preparatory GPC was conducted on a Toso chromatograph with a TSKgel G2000HHR column and toluene as a mobile phase. Analytical GPC was conducted on a Toso HLC-8020 chromatograph with a TSK gel G1000HXL column and toluene as a mobile phase. GPC with a triple-detection system was performed with a 2-PL gel mixed D

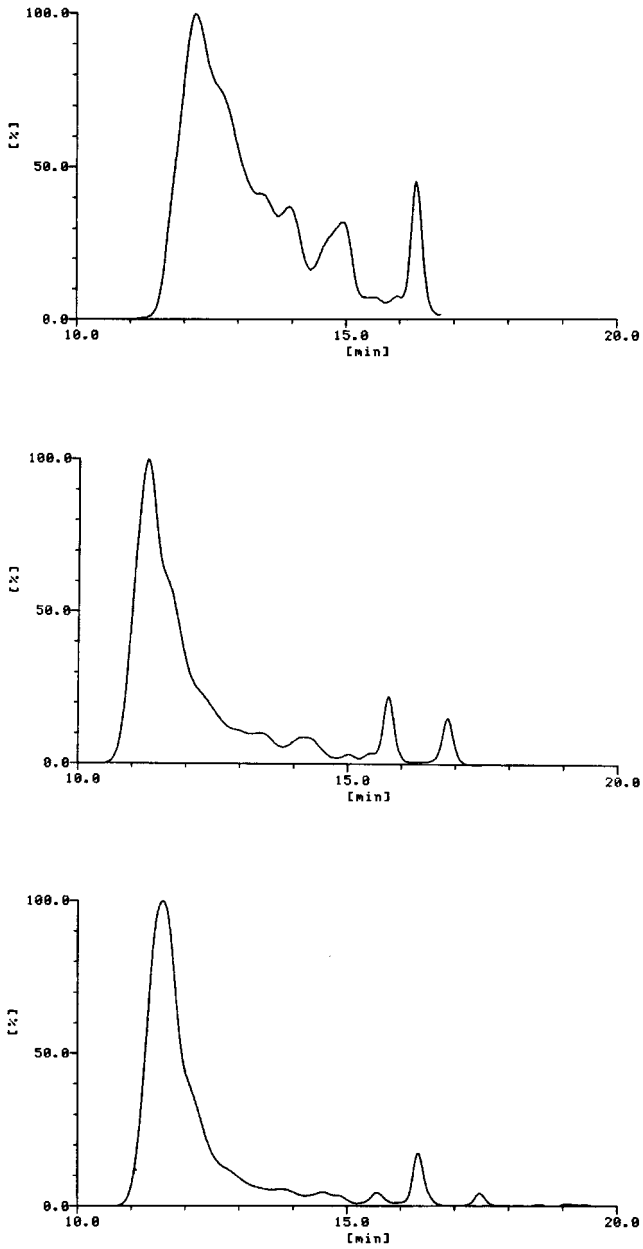

Figure 2. GPC analysis of the resins from the reaction of $(ViMe_2Si)_2O$ and $^{H}T_8$ at stoichiometries of 1:1 (top), 1.5:1 (middle), 2:1 (bottom).

column using THF as the eluent. The detection system consisted of a Viscotek model T60 that included a refractive index detector, a light scattering detector, and a viscosity detector. Gas chromatography was carried out on a Shimadzu chromatograph employing a Shimadzu GC-14A capillary column and a FID. The best separations were found with the following heating rates: 80 °C initial temperature ramping at 40 °C/min to 300 °C and hold there for 30 min. GC mass spectra studies (EI mode) were carried out on a Shimadzu GC-MS QP1000EX chromatograph employing a DB-5 column. The heating profile employed was as follows: 80 °C initial temperature ramping at 40 °C/min to 300 °C and held there for 30 min. Atmospheric pressure chemical ionization (APCI) MS studies were carried out on a PE Sciex triple quadrupole API 350 mass spectrometer operating at unit mass resolving power across the entire mass range (30−4500 Da). The APCI source was operated at ambient temperature (23 °C) and pressure while the quartz sprayer tube was held at 150 °C. The sprayer tube temperature was critically optimized such that solvent evaporation of the sprayed liquid solution could take place efficiently without inducing thermal decomposition of the

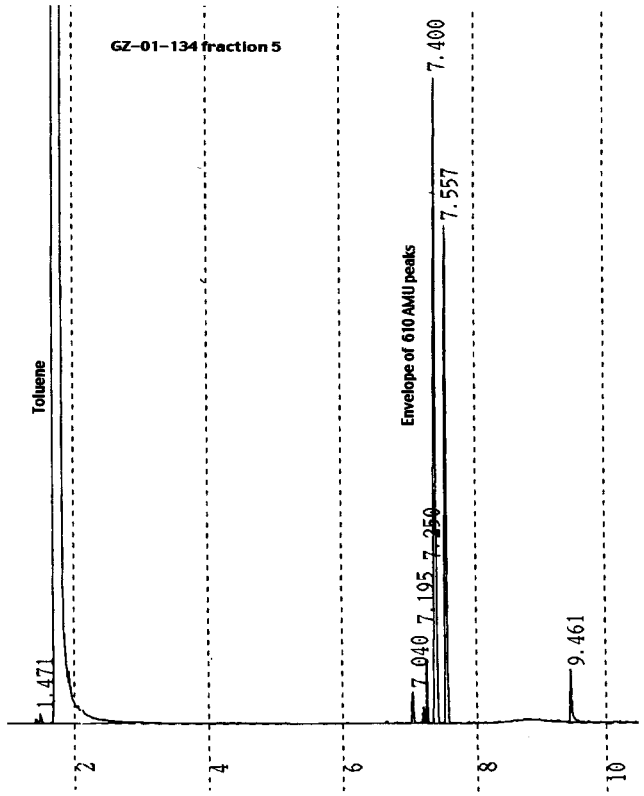

Figure 3. GC trace for fraction 5 from the reaction of $(ViMe_2Si)_2O$ and $^{H}T_8$. EI-MS signals were seen only for the peaks between 7.040 and 7.557 min of retention time and none for the peak at 9.461 min.

analytes. Solutions (50 ppm, wt/vol) of the samples were prepared in a 1:1 solution of MeOH/$CHCl_3$ from Fisher HPLC-grade MeOH and $CHCl_3$. The MeOH/$CHCl_3$ solutions containing the analytes were directly infused into the APCI ion source at a constant flow rate of 30 mL/min using a Harvard Apparatus (model 22) syringe pump, whereby solvent vaporization preceded ionization of the analytes. The APCI MS instrument was operated in the positive-ion mode. The nebulizing current applied to the nebulizing needle within the ion source was set to 1.5 mA, and the chemical ionization gas used was 1% NH_3 in Zero Air. The small amount of ammonia utilized in this custom chemical ionization gas was used to form stable ion-neutral complexes $[M+ NH_4]^+$ with high efficiencies and sensitivities. The $[M+ NH_4]^+$ ions are formed by undergoing low-translational-energy ion−molecule reactions with the chemical ionization plasma region of the ion source. In general, siloxanes do not cationize well with protons or N_2^+ ions as is normally observed for more polar materials analyzed by the APCI MS technique. The stable $[M+ NH_4]^+$ ion−neutral complexes formed in these studies were subsequently mass analyzed by the API 350 mass spectrometer and detected utilizing a channeltron detector operating at a voltage of 1800 V (gain = ca. 10^5), whereby 10 individual mass spectra were typically signal-averaged to provide a single summed mass spectrum. ^{1}H and ^{29}Si NMR spectra were recorded on a Bruker 300 MHz spectrometer. X-ray powder diffraction studies were conducted on a JEOL JDX-3530 diffractometer operated with graphite monochromator and Cu Kα radiation. For X-ray crystal structure analysis, a ruler-shaped crystal of the approximate dimensions of 0.6 × 0.34 × 0.07 mm was transferred to the goniostat of a Siemens Smart CCD diffractometer used with monochromated Mo−Kα radiation and cooled to 134 K. After Lp (Lorentz polarization factor) correction, 25 338 reflections survived out of which 7855 reflections were unique (Rint=0.0761), and 3207 reflections were considered observed ($I > 2\sigma I$). Corresponding crystal data are as follows: M_F $C_8H_{26}O_{13}Si_{10}$, M_W 611.19, triclinic, space group $P\bar{1}$, a = 9.567(1) Å, b = 12.156(2) Å, c = 12.497(2) Å, α = 74.78(1)°, β = 79.046(8)°, γ = 72.49(1)°, Z = 2, D_{calcd} = 1.529 g/cm^3. The structure solution was attempted by direct methods.[20] Atom form factors for neutral atoms were taken from the literature. From the resulting E-map, 20 meaningful peaks were taken to assemble a $[SiO_{3/2}]_8$ cage (T_8 cage). Full-matrix least squares refinement of the starting coordinates and subsequent difference Fourier syntheses revealed additional peaks which were picked to complete the molecule (Figure 12).

Scheme 1

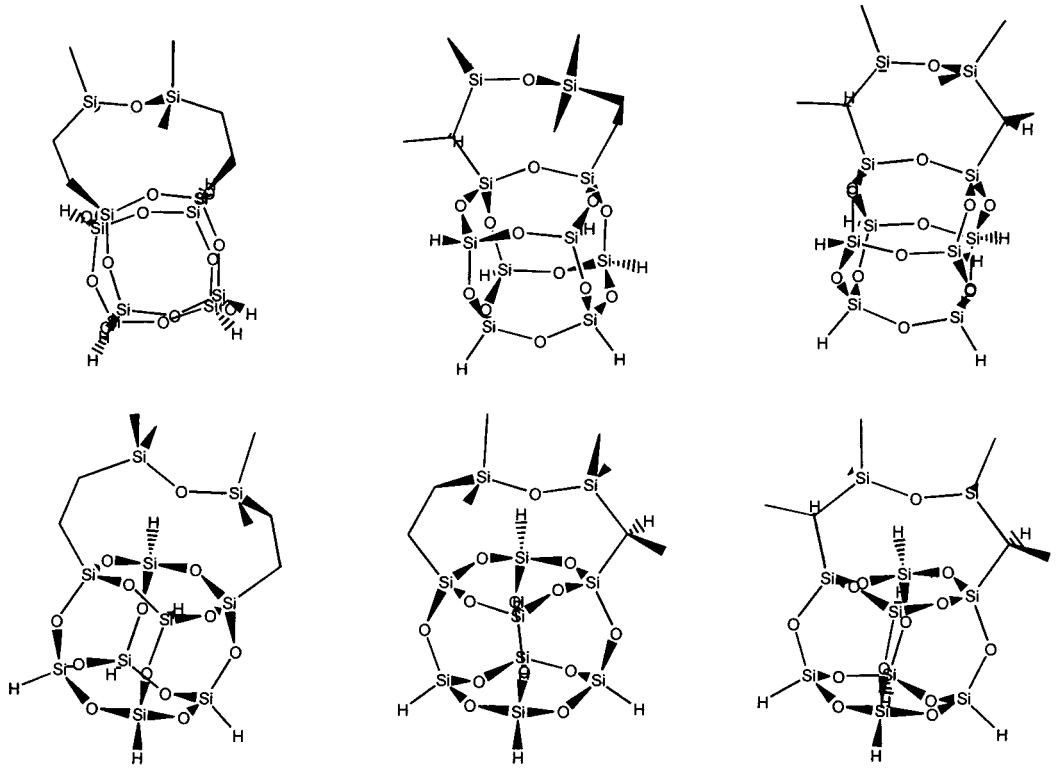

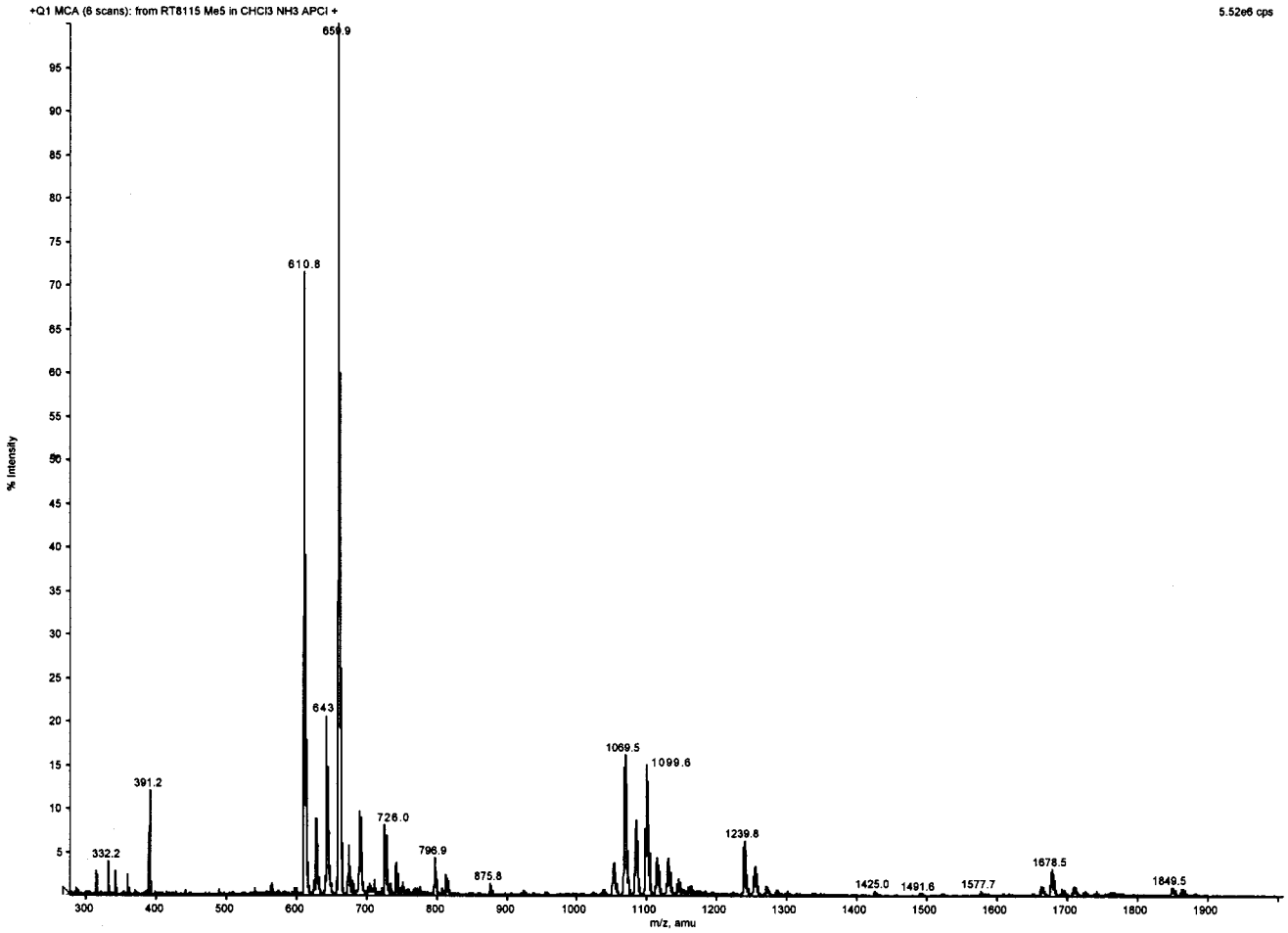

Figure 4. Positive-ion APCI mass spectrum of fraction 5 from the reaction of $(ViMe_2Si)_2O$ and $^HT_8$.

Large displacement parameters of the atoms of the bisethylidendi-methylsiloxy branch of the molecule made the introduction of a split atom model necessary. The calculations then converged with a final R_1 index of 0.1042 and with a goodness of fit of 1.490. Strong disorder of the branch atoms weakened the refinement: the "starred" atoms (see Supporting Information) could be only isotropically refined, and further possible positions for these atoms emerged from the F map but did not remain stable in the cause of the refinement. Hydrogen atoms could not be located and where not calculated in idealized positions since their pivot atoms showed too large atomic displacement parameters even at 134 K.

III. Discussion

Although there are many examples where alkenes have been reacted to H-functional cages by simple hydrosilation reactions, it is surprising that there have been no reports employing hydrosilation chemistry to "polymerize" H-functional cages with dienes. Despite the absence of any reports of these reactions, we have found them to be quite facile, and they easily afford soluble polymers. We have explored a range of dienes as well as a range of ratios of diene to cage to make a variety of soluble "resinous" materials. The range of polymeric materials prepared and their molecular weights are summarized in Table 2. We were surprised that soluble materials could be prepared from a variety of dienes even at ratios of linking groups to cages as high as 2:1. When we employed reactant ratios of 3:1, we consistently obtained large quantities of gel and were unable to isolate any materials from the reaction solution. Because of the large variety of different materials that were prepared in this work, the ensuing discussion will focus on the characterization of materials prepared from the reactions between the $^HT_8$ cages and $(ViMe_2Si)_2O$. Through this discussion, the reader will become familiar with all of the materials prepared in this study.

A. Gel Permeation Chromatography Characterization. Beginning with the reaction of $(ViMe_2Si)_2O$ and $^HT_8$ at a stoichiometry of 0.25:1, one sees predominantly low-molecular-weight species as the product by use of GPC analysis. This GPC trace is shown in Figure 1. The fraction labeled 6 corresponds to $^HT_8$ and was not characterized further. The fractions labeled 5, 3, and 1 were collected by preparatory GPC and characterized as described below.

From this separation it appears that fractions 5 and 3 are nearly monodisperse, whereas fraction 1 is at best a mixture of oligomeric materials. When the reaction stoichiometry is changed to 1:1, 1.5:1, or 2:1, the corresponding changes to the GPC traces are shown in Figure 2. It is interesting that as the ratio of the disiloxane to the cage is increased so too does the apparent molecular weight or size also increase. This was also the case when the universal calibration method and the light-scattering method were used to estimate

(20) Sheldrick, G. M. *SHELXL 97_2*, a program for crystal structure refinement; Sheldrick, G. M., Ed.; University of Göttingen: Göttingen, Germany, 1998.

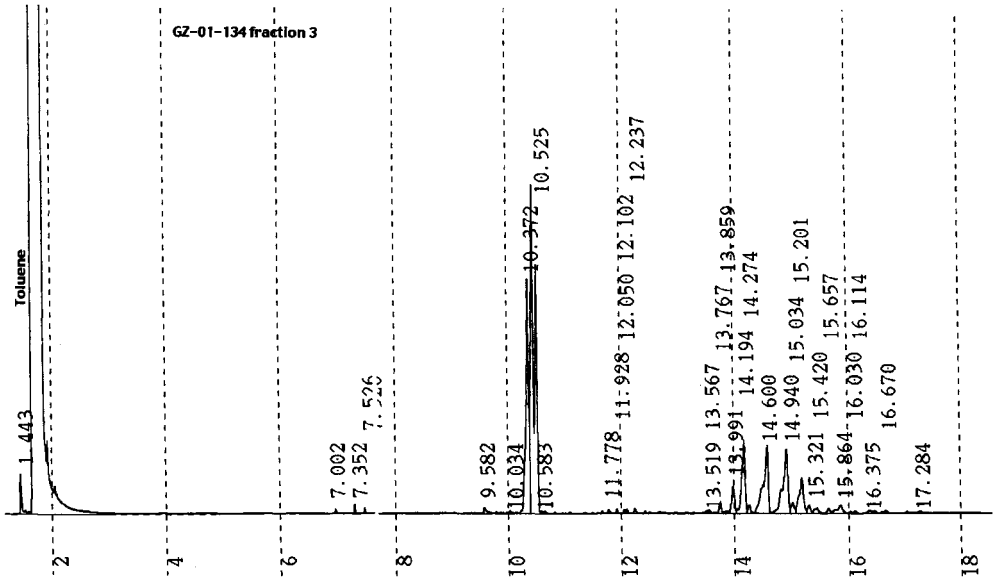

Figure 5. GC Trace for the fraction 3 product from the reaction of $(ViMe_2Si)_2O$ and $^{H}T_8$.

Scheme 2

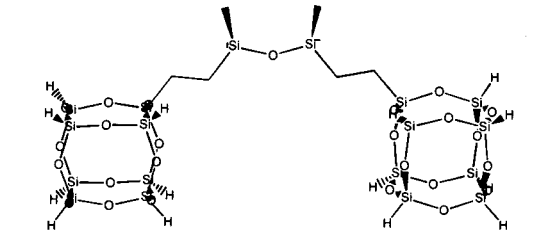

A

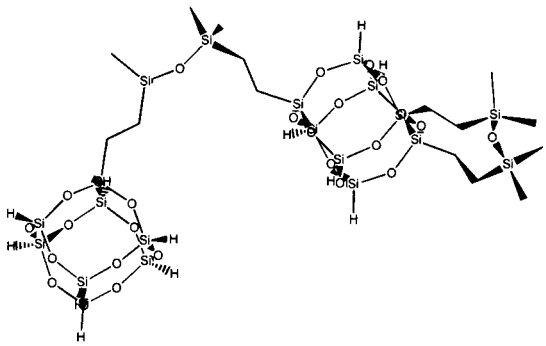

B

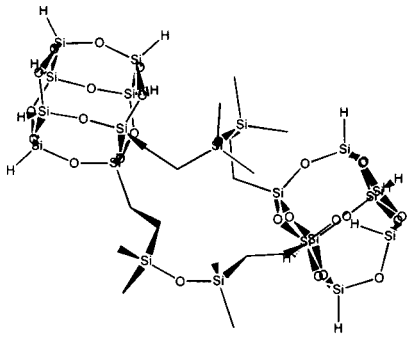

C

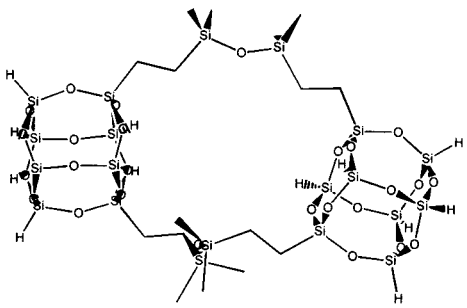

D

the molecular weight for these resin materials. The average radii of gyration R_g estimated by the light-scattering technique were 3.34 nm for the 1:1 stoichiometry resin, 6.33 nm for the 1:1.5 stoichiometry resin, and 10.91 nm for the 1:2 stoichiometry resin. Aside from the number- and weight-average molecular weight

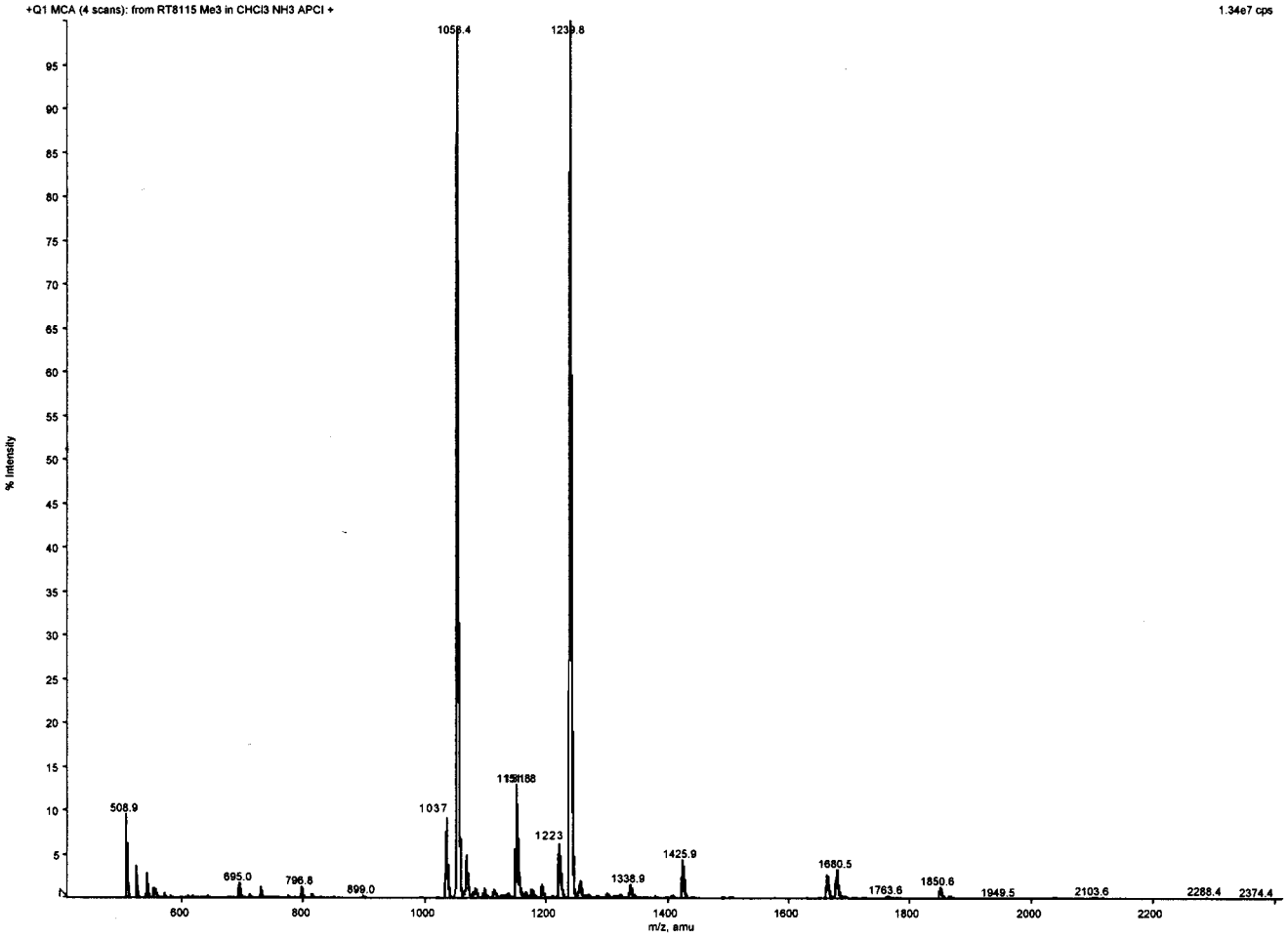

Figure 6. Positive-ion APCI mass spectrum of fraction 3 from the reaction of $(ViMe_2Si)_2O$ and $^HT_8$.

values listed in the table, the average value of the Houwink *a* parameter was also obtained. For the 1:2 stoichiometry resin, the relatively linear relationship was observed between intrinsic viscosity and molecular weight and the corresponding Houwink parameter *a* of 0.38 was obtained. For the 1:1 stoichiometry resin and the 1:1.5 stoichiometry resin, the Houwink parameters *a* in the molecular weight range over 15 000 showed the similar values, 0.39 and 0.33, as the 1:2 stoichiometry resin, whereas these two resins showed relatively constant intrinsic viscosity in the low-molecular-weight range, indicating the presence of spherical structures.

B. Gas Chromatography and Mass Spectral Characterization. The only materials with sufficient volatility to pass through a gas chromatography column and be ionized by "traditional" electron ionization (EI) GC-MS were the isolated fractions from the reaction stoichiometry of 0.25:1. Beginning with fraction 5, one sees a relatively clean GC-MS trace for this material from a toluene solution as shown in Figure 3. The five peaks in the GC-MS reconstructed chromatogram all have nearly identical mass spectra and measured molecular weights of 610 Da. One must be careful with this analysis since the upper mass limit of the GC-MS instrument employed was 1000 Da and the addition of one or more $^HT_8$ unit(s) to the 610 Da molecular weight affords a mass outside the scanable molecular weight range of the instrument. The 610 Da molecular weight corresponds to a formula of one $^HT_8$ cage and one of the disiloxane linking groups. The individual GC-MS peaks may well correspond to isomers of this composition which are most likely based on bonding position onto the cage (ortho and meta) and if the hydrosilation is α or β resulting in a silmethylene or silethylene linkage. The two most intense peaks account for 56% and 38% of the total peak areas within the envelope of all of the 610 Da species. If we assume that the $ViMe_2SiOSiMe_2$-Vi material is bidentate and therefore no free vinyl groups are present in these materials (an assumption that is supported by spectroscopic characterization, vide infra), there are six possible isomers as illustrated in Scheme 1. By employing relatively simple energetic calculation,[21] the cages with the disiloxane bidentate in ortho-positions are found to be consistently lower in energy. From these calculations, one would assume that the species with the highest abundances as seen in the GC are the ortho-substituted cages.

Due to the mass range limitation of GC-MS, an alternative mass spectrometry technique, atmospheric pressure chemical ionization (APCI) was also employed to analyze fraction 5. Numerous advantages exist when using the APCI MS technique compared to GC-MS. APCI MS is a "soft ionization" technique producing predominately intact cationized molecular ions leading to easy-to-interpret mass spectra (see Experimental Section). The samples were prepared in 1:1 MeOH/$CHCl_3$ solutions and directly infused into the mass

(21) *CS Chem 3D Pro*; CambridgeSoft Corporation: Cambridge, MA, 1998.

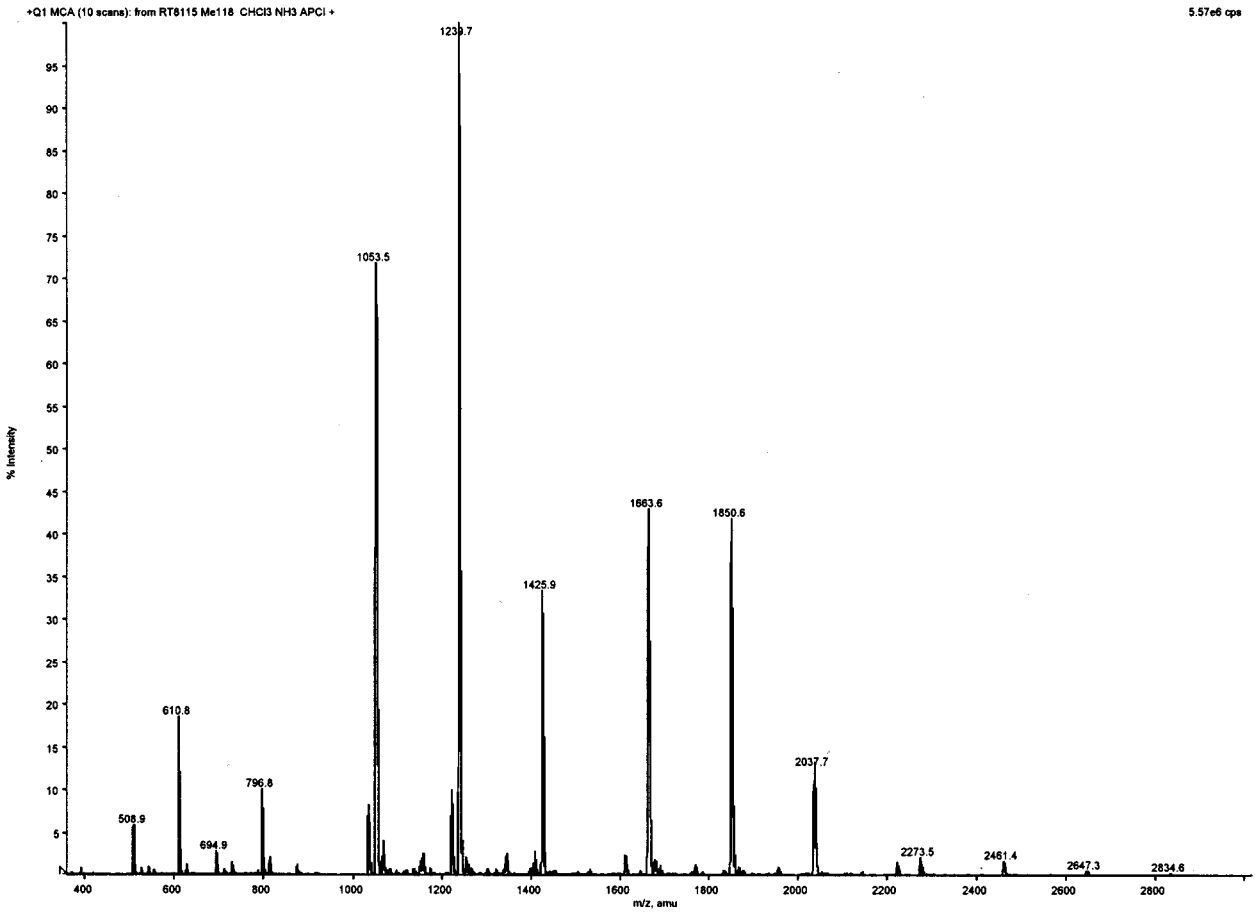

Figure 7. Positive-ion APCI mass spectrum of fraction 1 from the reaction of $(ViMe_2Si)_2O$ and $^{H}T_8$.

spectrometer without the use of an HPLC or GPC column, and a wide mass range (30−4500 Da) was achievable using this mass spectrometer. The presence of 1% ammonia gas in the air which was used as the CI gas in the APCI MS studies was necessary to ammoniate the silicones $[M+NH_4]^+$ present with high efficiencies and sensitivities. The positive-ion APCI mass spectrum of fraction 5 is shown in Figure 4. The various cations attached to the silsesquioxanes species present in the APCI mass spectra of fractions 5, 3, and 1 must be taken into account when interpreting the MS results. As a specific example the *m*/*z* 610 ion detected by GC-MS for the structure corresponding to one $^{H}T_8$ cage and one disiloxane linking group was observed as four ions by APCI. In addition to the $[M+NH_4]^+$ ion (*m*/*z* 628), the $[M+H]^+$ (*m*/*z* 611), $[M+MeOH+H]^+$ (*m*/*z* 643), and $[M+MeOH+NH_4]^+$ ions (*m*/*z* 660) were also observed. The observation of the later two ions with the presence of neutral methanol attached to either the protonated or ammoniated molecular ion indicates that incomplete desolvation occurred within the ion source prior to mass analysis.

From the interpretation of the APCI MS data in Figure 4, one sees that "parent ions" with molecular weights in excess of 1000 Da are observed, indicating that there are species present that are beyond the upper mass limit of the EI GC-MS instrument. Although one cannot accurately relate the APCI MS peak intensities to absolute analyte concentrations, the ion intensities in Figure 4 are observed to decrease as the series progresses from $1^{H}T_8$ and $1(ViMe_2Si)_2O$ (610 Da) to $2^{H}T_8$ and $1(ViMe_2Si)_2O$ (1034 Da) to $2^{H}T_8$ and $2(ViMe_2Si)_2O$ (1220 Da), with other ions of very small intensity corresponding to $1^{H}T_8$ and $2(ViMe_2Si)_2O$ (796 Da), $2^{H}T_8$ and $3(ViMe_2Si)_2O$ (1406 Da), $3^{H}T_8$ and $2(ViMe_2Si)_2O$ 1644 (Da), and $3^{H}T_8$ and $3(ViMe_2Si)_2O$ (1830 Da). It is interesting that even in this lowest molecular weight fraction prepared from GPC fractionation, a wide variety of species are still detected by APCI MS with masses as large as 1830 Da.

Turning to fraction 3, the next higher in molecular weight materials, nothing was detected by GC-MS with the 1000 Da upper mass limit of the instrument. Some materials do have sufficient volatility, however, to pass through a GC and can be observed by flame ionization detection (FID). The corresponding GC FID trace for this fraction is shown in Figure 5. From this analysis based on the relative retention times in both the GC and the GPC, it is likely that these peaks between the retention time of 10.37 and 10.52 min correspond to 2 $^{H}T_8$ cages linked by one $(ViMe_2Si)_2O$ group. The total summed peak area for these peaks is 58%, ignoring the peak areas due to the solvent in the GC trace. Candidate structures for this material are shown in Scheme 2A. Again, one would expect three isomers depending on the hydrosilation being both α or *β* or a mixture of these (α, α; α, *β*; or *β*, *β*) within one molecule, which corresponds to the number of peaks in the GC analysis. There is another set of peaks at a retention times between 13.5 and 15.2 min that account for 36% of the total peak area, neglecting the solvent. These are most likely isomers of the general composition of two $^{H}T_8$ cages linked by

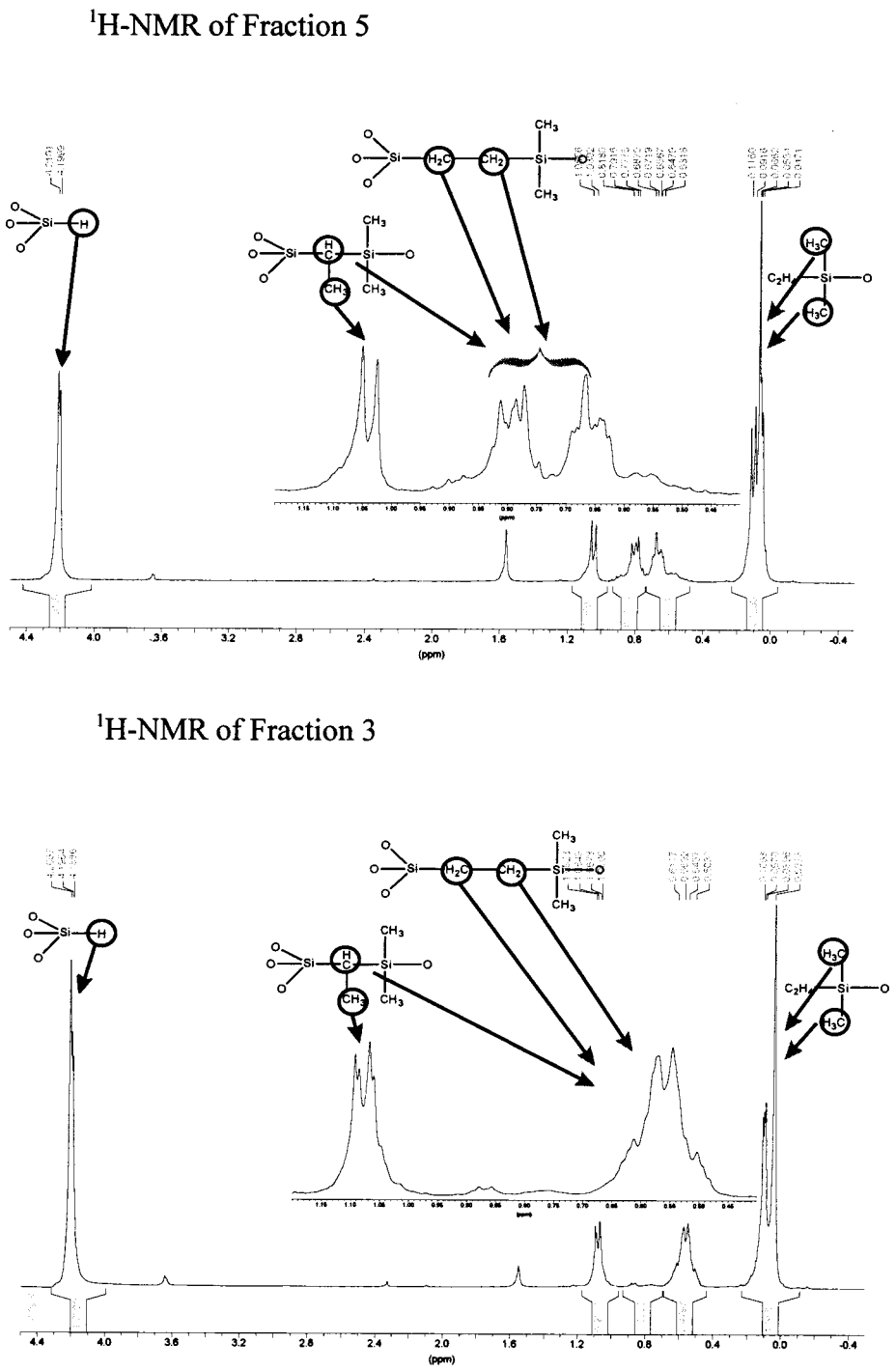

Figure 8. ^{1}H NMR spectra of fractions 5 and 3 from the reaction of $(ViMe_2Si)_2O$ and $^HT_8$.

two $(ViMe_2Si)_2O$ groups. For this composition, there can be many isomers depending on the following: if the disiloxane is bidentate or bridging between two cages, the relative locations of binding on the individual cages, and if the hydrosilation was at the α or β position. Some, but not an exhaustive listing, of the possible isomers are drawn in Scheme 2B−D.

The assumptions of the structures based on the GC peaks and their retention times are supported by results from the APCI MS analysis of fraction 3. The positive-ion APCI mass spectrum of fraction 3 is shown in Figure 6. Although one cannot accurately quantify the results of this analysis, the two most abundant species are 2^HT_8 and $1(ViMe_2Si)_2O$ (1034 Da) and 2^HT_8 and $2(ViMe_2Si)_2O$ (1220 Da), with the $[M+NH_4^+]$ being the strongest peaks seen in the analysis. Other ions of very small intensity corresponding to 2^HT_8 and $3(ViMe_2Si)_2O$ (1406 Da), 3^HT_8 and $2(ViMe_2Si)_2O$ (1644 Da), and 3^HT_8 and $3(ViMe_2Si)_2O$ (1830 Da) are also seen.

In looking at the highest molecular weight fraction, fraction 1, as anticipated, there are no species detected by either GC-MS or GC analysis. So as with higher molecular weight polymeric materials only GPC analysis and mass spectrometry provide any insights into the distribution of molecular weights present within the fraction. The APCI MS analysis of this fraction provides insights into the higher molecular weight materials present in the actual polymers, as the analysis shows

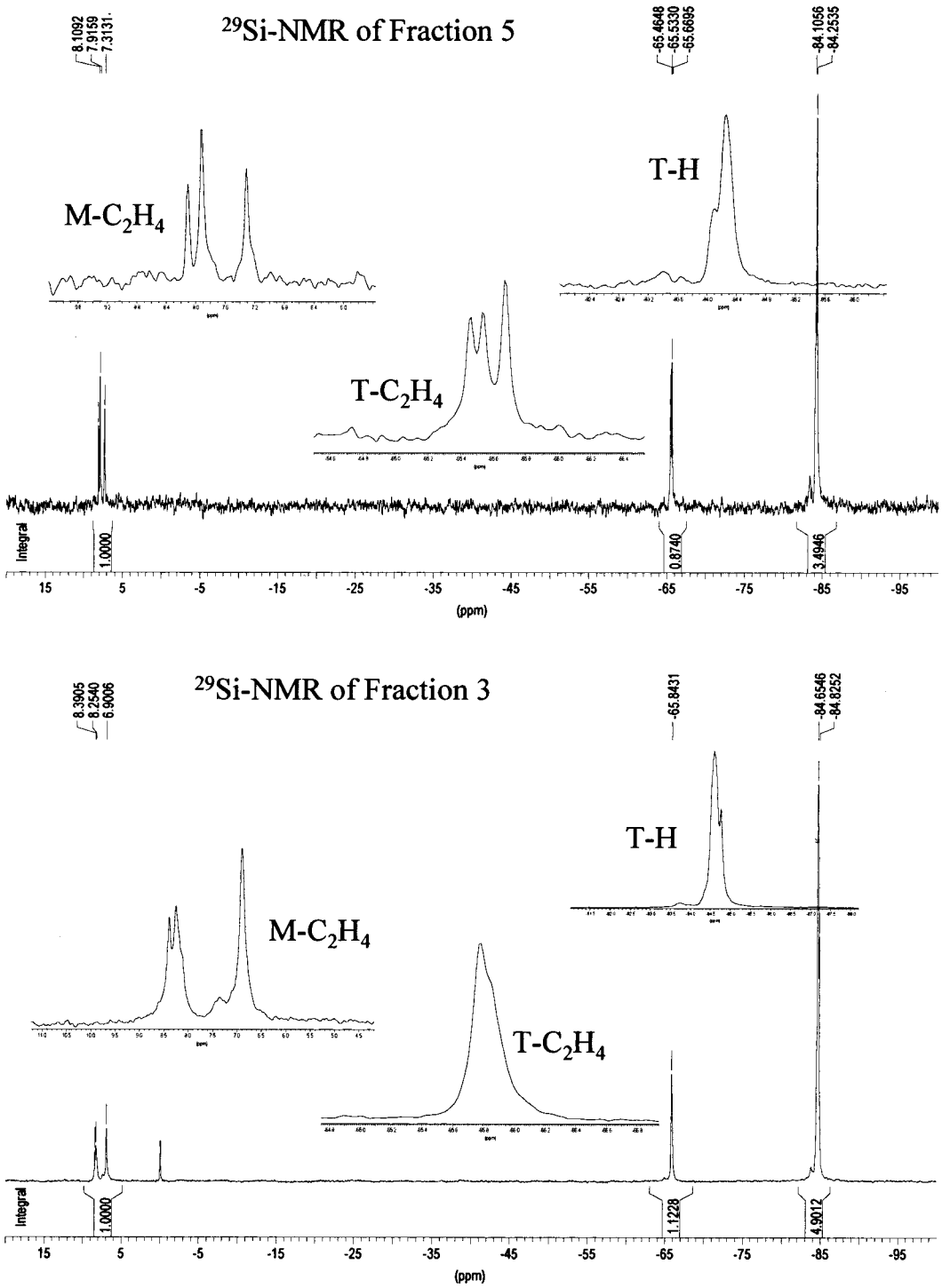

Figure 9. ^{29}Si NMR spectra of fractions 5 and 3 from the reaction of $(ViMe_2Si)_2O$ and $^{H}T_8$.

quite a range of materials present over the ratios of $(^{H}T_8)_n((ViMe_2Si)_2O)_y$ where y ranges from $n - 1$ to $n + 2$ and $n \leq 4$. The positive-ion APCI mass spectrum of fraction 1 is shown in Figure 7. From the GC-MS, GC, and APCI MS studies, one can arrive at the following conclusions starting with the smaller molecules. Fraction 5 is predominantly composed of a material with one $^{H}T_8$ cage and one $(ViMe_2Si)_2O$ linking group. We cannot discern if the disiloxane is mono- or bidentate on the cage, since both of these structures are isobaric by MS analyses. We also see that this fraction contains some larger oligomeric materials by APCI MS. It is believed that these multiple peaks observed in the GC trace are due to isomers of the basic formula (one cage + one link); a variety of these structures are drawn in Scheme 1. Fraction 3, by GC and APCI MS analyses, is a mixture of predominantly two $^{H}T_8$ cages and one $(ViMe_2Si)_2O$ linking group, with three possible isomers, along with two $^{H}T_8$ cages and two $(ViMe_2Si)_2O$ linking groups. By APCI MS, fraction 1 is not a pure compound but rather a mixture of intermediate molecular weight materials that provide useful insights into the "structure" and key building block moieties of the bulk resin, as materials covering a range of compositions: of $n(^{H}T_8)$ cages and $y(ViMe_2Si)_2O$ linking groups where y ranges from $n - 1$ to $n + 2$ and $n \leq 4$ are observed. Although the

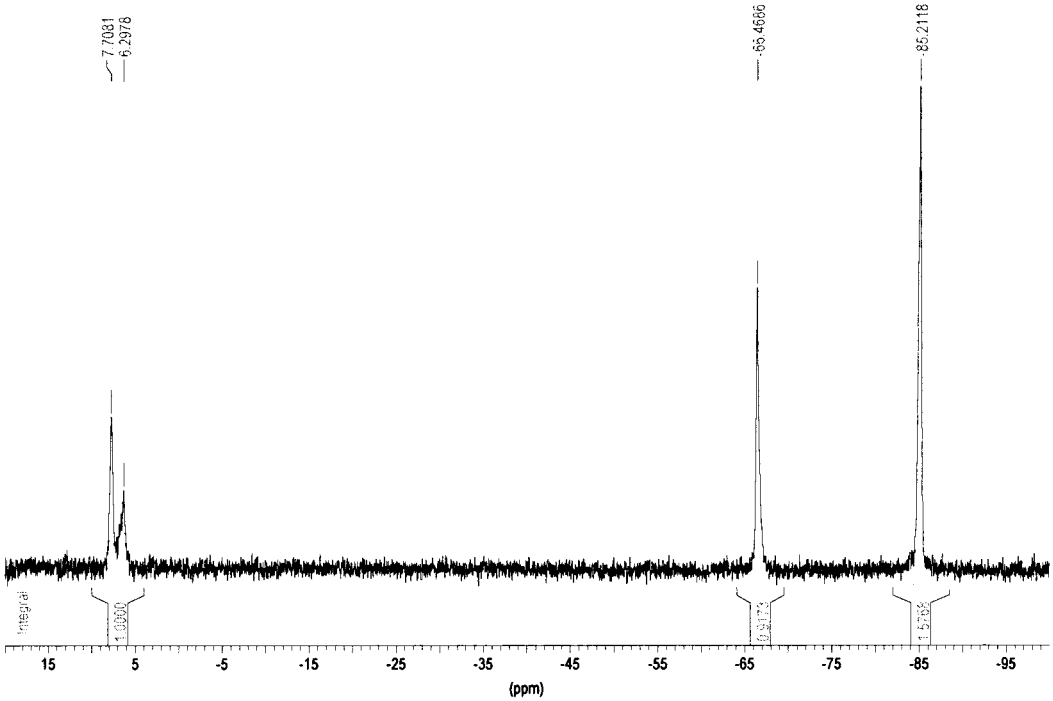

Figure 10. ^{29}Si NMR spectrum of the polymer from the reaction of $(ViMe_2Si)_2O$ and $^{H}T_8$ at a stoichiometry of 1.5:1.

Table 3. ^{29}Si NMR Characterization Summary

linking group Vi−L−Vi	link:cage	^{29}Si NMR assign[a] (descrip.; chem. shift(ppm); integr.)
$-Me_2SiOSiMe_2-$	1:1	^{Et}M (2s; 8.727, 7.421; 2.39); ^{Et}T (s; −65.281; 2.36); ^{H}T (s; −84.070; 5.64)
	1.5:1	^{Et}M (2s; 7.708, 6.298; 3.21); ^{Et}T (s; −66.469; 2.94); ^{H}T (s; −85.212; 5.06)
	2:1	^{Et}M (2s; 8.741, 7.421; 3.89); ^{Et}T (s; −65.174; 4.04); ^{H}T (s; −83.868; 3.96)
$-Ph_2SiOSiPh_2-$	1:1	^{Ph2Et}M (m; −8.835, −9.590, −10.262, −20.903; 2.16) ^{Et}T (3s; −64.762, −65.780, −66.561; 2.03); ^{H}T (s; −84.366; 5.97)
$-(Me_2SiO)_7-$	1:1	^{Et}M (2s; 8.075, 6.701; 2.07); ^{Me2}D (3s; −21.313, −21.502, −21.933; 6.86); ^{Et}T (s; −65.813; 2.02); ^{H}T (s; −84.615; 5.98)
$-(Me_2SiO)_{10}-$	1:1	^{Et}M (2s; 8.048, 6.728; 2.68); ^{Me2}D (3s; −21.461, −21.583, −22.014; 8.08); ^{Et}T (s; −65.867; 2.63); ^{H}T (s; 84.667; 5.37)
	2:1	^{Et}M (2s; 8.621, 7.438; 4.42); ^{Me2}D (2s; −20.992, −21.405; 12.55); ^{Et}T (2s; −65.078, −65.419; 4.12); ^{H}T (s; −83.844; 3.88)
$-(C_6H_4)-$	1:1	^{Et}T (2s; −66.600, −70.829; 2.43); ^{H}T (3s; −83.382, −83.786, −84.217; 5.56)

[a] Where $^{Et}T = (C_2H_4)SiO_{3/2}$, $^{H}T = HSiO_{3/2}$, $^{Me2}D = Me_2SiO_{2/2}$, $^{Et}M = (C_2H_4)Me_2SiO_{1/2}$, $^{Ph2Et}M = (C_2H_4)Ph_2SiO_{1/2}$, s = singlet, 2s = two singlets, 3s = 3 singlets, and m = multiplet.

compositional information is in hand, little can be said about the detailed three-dimensional structural nature of these compositions, and for this, we must turn to spectroscopic studies.

C. Nuclear Magnetic Resonance Characterization. Insights into the structure of the different fractions are obtained from ^{1}H NMR spectroscopy shown in Figure 8. The compositional information from the integration of the proton NMR spectra are as follows. Fraction 5: $(Si-H)_6$, $(-C_2H_4-)_2$, $(Si(CH_3)_2)_2$, this is consistent with the GC-MS and APCI MS results that indicated an atomic composition corresponding to one cage and one linking group. The fact that no free olefin is seen in this ^{1}H NMR spectrum supports the belief that the linking group is bidentate on the $^{H}T_8$ cage. The integration of the ^{1}H NMR spectrum of fraction 3, $(Si-H)_{6.5}$, $(-C_2H_4-)_{1.4}$, $(Si(CH_3)_2)_{1.5}$, is again consistent with the mass spectral results that indicate a mixture of two cages and one linking group along with two cages and two linking groups. The ^{1}H NMR spectral integration indicates that fraction 1 is roughly as follows: $(Si-H)_6$, $(-C_2H_4-)_2$, $(Si(CH_3)_2)_2$. If we focus on the spectra from fractions 5 and 3, we can see some very distinct differences between the two spectra aside from the integration. First, the spectral region for bridging organic linkage between the disiloxane and the cage between 0.6 and 1.2 ppm indicates that there is a substantial amount of α-hydrosilation product. From the integration, one arrives at a value of 36% α to 64% *β* in this fraction 5 material. There is not much additional information from the Si-*H* region, but it is interesting that the $Si-CH_3$ region is divided into one main resonance with four smaller resonances, and some are dramatically shifted to lower fields in fraction 3. For fraction 3, there is much less information from the ^{1}H NMR spectra due to the broadening of the lines; however, one still sees a substantial amount of α-hydrosilation product (42% α to 58% *β*). The lower field resonances associated with the $Si-CH_3$ region are now even more separated from the main resonance.

The ^{29}Si NMR of fractions 5 and 3 are shown in Figure 9. For fraction 5, the integration is consistent with a

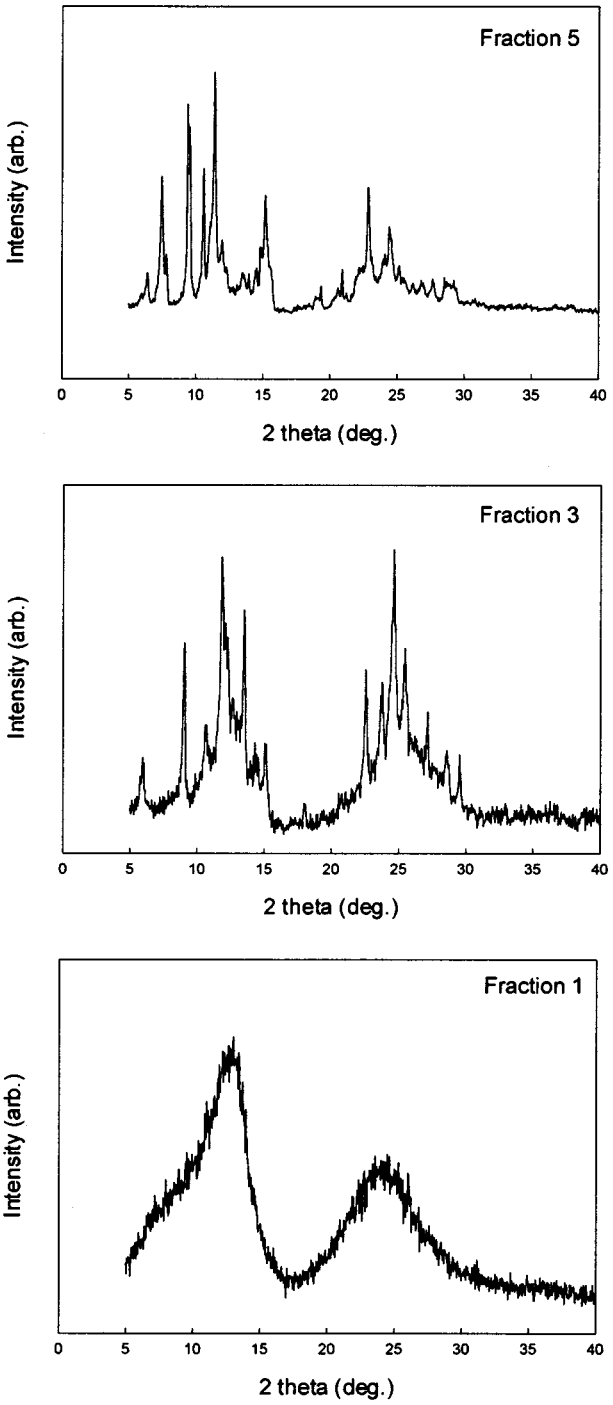

Figure 11. WAXD patterns of fractions 5, 3, and 1 from the reaction of $(ViMe_2Si)_2O$ and $^{H}T_8$.

formula of $(O_{3/2}Si-H)_{6.2}$, $(O_{3/2}Si-C_2H_4-)_{1.6}$, $(O_{1/2}Si(C_2H_4)-(CH_3)_2)_{1.8}$, which is similar to that of the proton spectra that gave the ratios of $(O_{3/2}Si-H)_6$, $(O_{3/2}Si-C_2H_4-)_2$, $(O_{1/2}Si(C_2H_4)(CH_3)_2)_2$. Other information from the ^{29}Si NMR is that the $T-C_2H_4$ (substituted cage) region of the spectrum and the $M-C_2H_4$ region show three resonances each. It is simple to rationalize two resonances, one each for the α- and β-hydrosilation isomers, but the assignment of all three resonances is not obvious. Also interesting is the relative insensitivity of the T−H resonance to what is happening elsewhere on the cage. The T−H region shows only two resonances while this fraction could contain a number of environments about the silicon (for example, see Structure 2) as well as positions around the cage. Once one group is

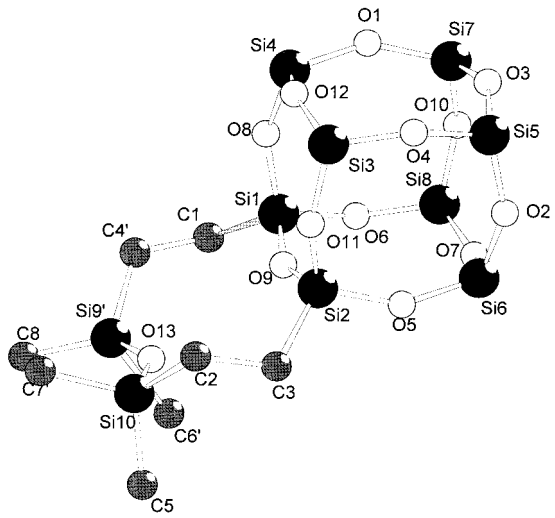

Figure 12. Diamond representation of the molecular structure of $(HSiO_{1.5})_6(O_{1.5}SiC_2H_4SiMe_2O_{0.5})_2$ in one possible conformation.

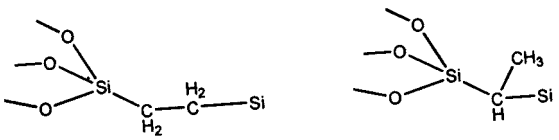

structure 2

hydrosilated to the cage there are then three positions "ortho (Or)" to that group, three positions "meta (M)" and one "para (Pa)" to the monosubstituted cage where a second substitution can take place, with ortho and meta being statistically favorable.

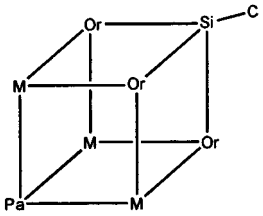

structure 3

For fraction 3, the integration is consistent with a formula of $(O_{3/2}Si-H)_{6.6}$, $(O_{3/2}Si-C_2H_4-)_{1.5}$, $(O_{1/2}Si(C_2H_4)-(CH_3)_2)_{1.4}$, which is close to the results from ^1H NMR. It is interesting that the number of the resonance in $M-C_2H_4$ and T−H regions are very similar to that of fraction 5, but the $T-C_2H_4$ region shows simply one resonance with a shoulder, although the reasons for these similarity and difference are not understood.

For fraction 1, there is no additional structural information, as the spectra of this now more complicated mixture of materials resembles that of the high-molecular-weight polymers that we discuss next.

The ^{29}Si NMR spectra were recorded as $CDCl_3$ solutions for the polymers. The spectra of the polymeric product from the stoichiometry of $1.5(ViMe_2Si)_2O$ linking groups per $^{H}T_8$ cage is shown in Figure 10, and all of the ^{29}Si NMR spectra for the polymeric materials are summarized in Table 3. We where initially surprised with the relative simplicity of the spectra. It is obvious

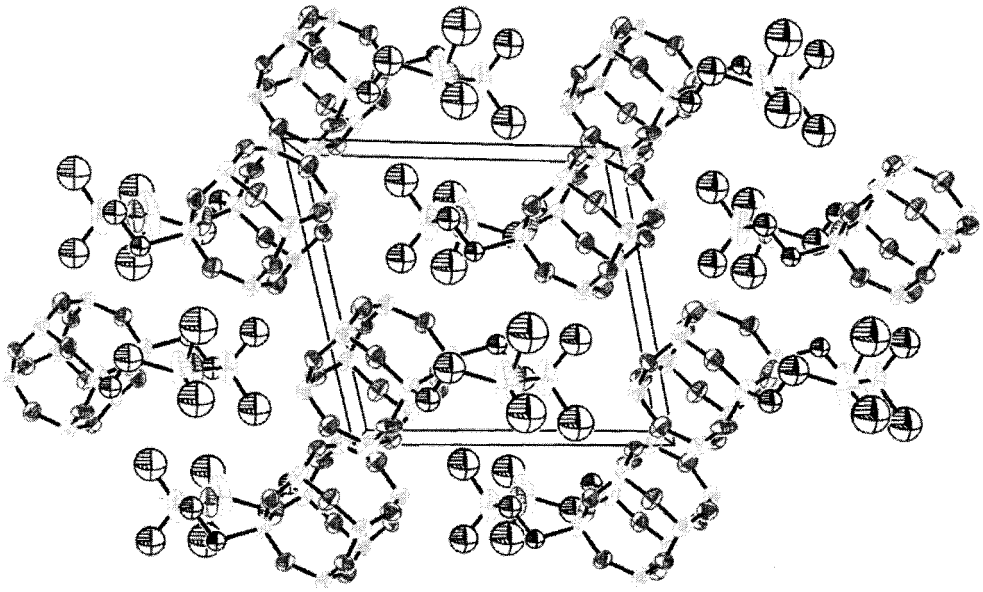

Figure 13. Packing diagram of $(HSiO_{1.5})_6(O_{1.5}SiC_2H_4SiMe_2O_{0.5})_2$ shown in Figure 12.

that these materials contain a number of environments about the silicone as described above. Taking this together with the fact the product stoichiometries are at best only averages, meaning that in any one molecule there will be a variety of cages with different numbers and positions of substitution, we did not anticipate that the spectra would be dominated by sharp single peaks but would rather be composed of broad multiplets reflecting the multiplicity of Si environments which is often seen in the spectra of organosilsesquioxanes prepared from the hydrolytic condensation of $RSiX_3$ even at these low (300 MHz) fields.

The ^{29}Si NMR spectra of these materials show sharp single resonances (as is shown in Figure 10 as an example) for all of the materials studied, irrespective of the type of linking group or the number of linking groups per cage. This is likely a reflection of the field employed and that the bond geometry or angles about the different silicon environments are nearly always constant. As an example, all T silicon species are part of a completely condensed T_8 cage. It is likely that the sharp "single" resonances seen in the ^{29}Si NMR spectra of even the very high-molecular-weight polymers are due to the relatively constant silicon bond geometries found in these materials. Since typical high-molecular-weight silsesquioxanes that are derived from the hydrolysis of silane monomers show broad ^{29}Si NMR resonances even at these low field strengths for the T silicons, we can therefore infer that there are a variety of bond geometries about the silicon atoms in classical silsesquioxane materials.

D. X-ray Analysis. The wide-angle X-ray diffraction and scattering patterns from powdered samples of the isolated fractions are shown in Figure 11. Although the other characterization techniques have shown that these fractions are not composed of unique molecular materials, the WAXD patterns of fractions 5 and 3 show patterns indicative of crystalline materials. The large number of diffraction lines may indicate the presence of many crystalline species or that there are many polymorphs (due to preparation of the powdered solid sample) of the relatively few materials present. It is interesting to compare the diffraction pattern changes between fractions 3 and 1. The diffraction pattern of fraction 1 is surprisingly similar to the WAXS patterns that are typically seen for silicone resin materials, two broad features centered at ca. 12.5 and ca. 24° 2θ.[22−25] These angles correspond to the distances of 0.7 and 0.4 nm, respectively.

For fraction 5 when more careful sample preparation was carried out (slow evaporation of dilute toluene solution), single crystals were obtained. We carried out X-ray single-crystal analysis of one of these crystals in an effort to unequivocally determine its structure. Only two organylheptahydro octasilsesquioxanes of the pseudocubane type are structurally characterized (*n*-hexyl-,[26] phenyl-[27]); no reports are given where one Si−O−Si edge of a Si_8O_{12} cube is also part of a condensed macrocycle. The core of the molecule is a T_8 unit $[(SiO_{3/2})_2(HSiO_{3/2})_6] = [H_6Si_8O_{12}]$ where two adjacent Si atoms of the Si cube are linked by a dimethylsiloxy-bisethylidene branch, as shown Figure 12 together with an expanded lattice view shown in Figure 13. The pseudocubane topology of Si_8O_{20} [28] in silicates and R_8-Si_8O_{12} [29] in silsesquioxanes is well-established: the observed Si−O distances, 0.1612 (13) nm, as well as the large bond angles at the bridging oxygen atoms, 148.9 (11)°, fit well with the datasets reported in the literature.[30]

(22) Mi, Y.; Stern, S. A. *J. Polym. Sci., Part B: Polym. Phys.* **1991**, *29*, 389−93.
(23) Xie, Z.; He, Z.; Dai, D.; Zhang, R. *Chin. J. Polym. Sci.* **1989**, *7*, 183−8.
(24) Zhang, X.; Shi, L.; Huang, C. *Chin. J. Polym. Sci.* **1987**, *5*, 353−8.
(25) Adrianov, K. A.; Zhdanov, A. A.; Levin, V. Y. *Ann. Rev. Mater. Sci.* **1978**, *8*, 313−26.
(26) Calzaferri, G.; Imhof, R.; Tornroos, K. W. *J. Chem. Soc., Dalton Trans.* **1994**, 3123−8.
(27) Calzaferri, G.; Marcolli, C.; Imhof, R.; Tornroos, K. W. *J. Chem. Soc., Dalton Trans.* **1996**, 3313−22.
(28) Moke′eva, U. I.; Golovastikov, N. I. *Dokl. Akad. Nauk SSSR* **1966**, *167*.
(29) Rebrov, E. A.; Tebeneva, N. A.; Muzafarov, A. M.; Ovchinnikov, Y. E.; Struchkov, Y. T.; Strelkova, T. V. *Izv. Akad. Nauk SSSR, Ser. Khim.* **1995**, 1332.
(30) Auner, N.; Ziemer, B.; Herrschaft, B.: Ziche, W.; John, P.; Johann, W. *Eur. J. Inorg. Chem.* **1999**, 1087.

Although it is not possible to identify and quantify the numbers of the linking groups that are on one cage versus linking two cages from the NMR spectroscopy or GC analysis of the high-molecular-weight materials, it is safe to say from this detailed analysis of the low-molecular-weight oligomeric species that in polymeric materials some fraction of the linking groups (here, disiloxane) are bidentate to an individual cage. This is the most probable reason that the materials even with two linking group per cage ratio are still soluble.

The XRD results of the high-molecular-weight resins from the reaction of $(ViMe_2Si)_2O$ and $^{H}T_8$ at a stoichiometry of 1:1, 1.5:1, and 2:1 are shown in Figure 14. In these patterns one sees three peaks at two θ positions of ∼8, ∼12.5, and ∼23° corresponding to equivalent Bragg distances of ∼1.1, ∼0.7, and ∼0.4, respectively. This is an indication of the presence of specific periodic features in the materials. The broad high-angle peak which corresponds to a distance of about 0.4 nm most likely corresponds to the Si−O−Si repeating unit within the structures since this broad feature is found in most all amorphous silicone-based materials. Interestingly there are two peaks at 8° and 12.5° and the relative intensity of the peak at 8° to the peak at 12.5° increase when the stoichiometry is changed from 1:1 to 2:2, whereas the patterns typically seen for silicone resin materials show only one broad peak around the similar two theta range.[6,11,22−25] This implies that the materials formed relatively ordered packing in solid state to show two different periodicities. The Bragg's distances of 0.7 and 1.1 nm are similar in size to the cage dimension and the scale of one cage plus one linking molecule L, respectively, as shown in Figure 15. It is tempting to assign these peaks to some of the repeat units shown in Figure 15; however, we feel that this is very misleading since we see very little changes in the WAXS patterns when we employ longer linking groups, see Table 4, and employing these distances, it is also difficult to explain the seemingly sequential changes seen in the scattering patterns shown in Figure 14 that take place due to the addition of more linking groups to the material's composition. Detailed structural and morphological study based on much more theoretical aspect such as the analysis of the radial distribution function is beyond the scope of this work. At this time, until more detailed scattering work is completed, the origin of these WAXS peaks cannot be determined with certainty.

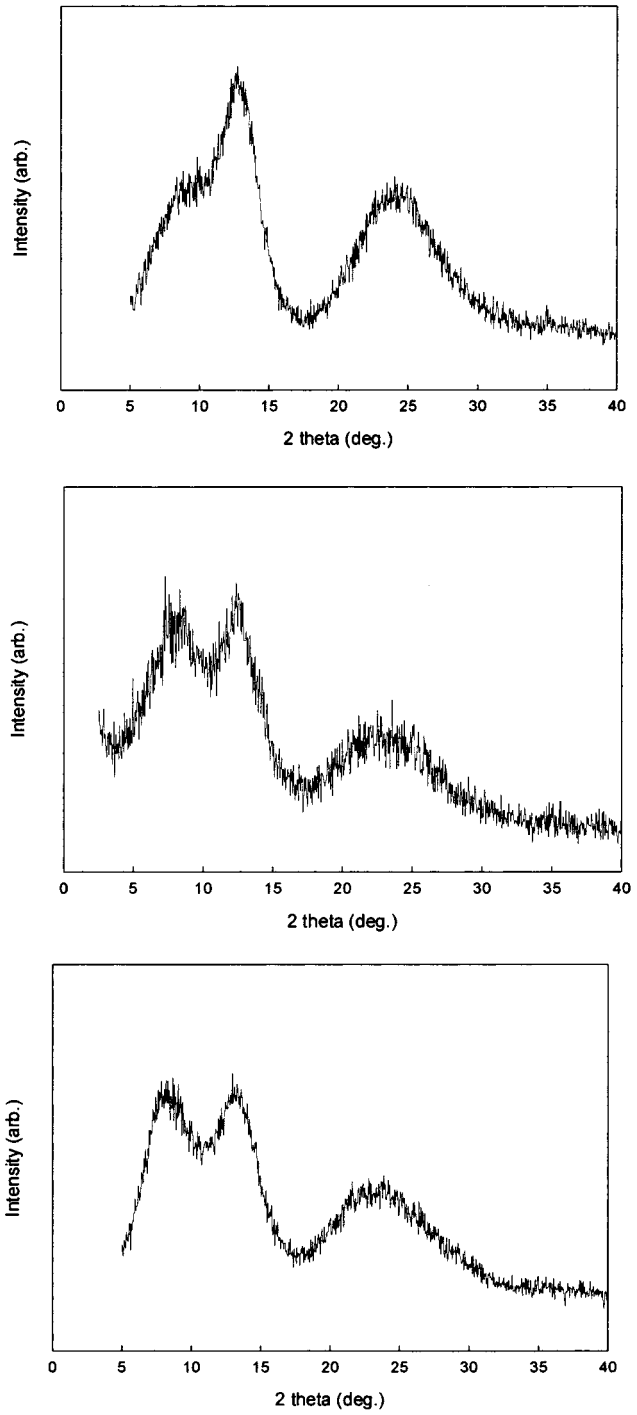

Figure 14. WAXS patterns of the resins from the reaction of $(ViMe_2Si)_2O$ and $^{H}T_8$ at stoichiometries of 1:1 (top), 1.5:1 (middle), and 2:1 (bottom).

IV. Summary

In this study, we have demonstrated a relatively simple method for the preparation of silicone-based polymers that contain completely condensed cages (T_8) as integral components of the material structure. The characterization of these polymers indicates that with the right stoichiometry they can have high molecular weights (M_w of 1.2 million), that they are soluble in most common organic solvents, and that the T_8 cages remain intact even in the high-molecular-weight materials. We have shown that the linking groups are all bidentate but are a mixture linking two cages as well as chelating to a single cage. Interpretation of the spectroscopic analysis and of these polymers is aided greatly by the corresponding characterization of model, small molecules. The small molecule characterization was done with gas chromatography (GC), GC coupled with mass spectrometry detection (GC-MS), and APCI MS to arrive at atomic weights, structural formulas, and structural isomers in these models. In one case, an unequivocal structure was assigned from a single-crystal X-ray diffraction study. The techniques that were found to be most useful in understanding the three-dimensional structures of the high-molecular-weight polymers were NMR and GPC. The ^{29}Si NMR spectra of these polymers are much simpler than those that are obtained from traditional silicon resins made from the hydrolysis of

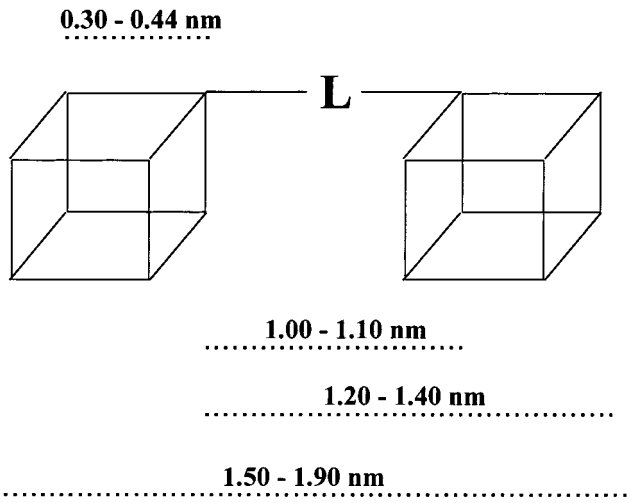

Figure 15. Average "repeating distances" calculated for the polymeric materials from models with sterically minimized structures.

Table 4. WAXS Characterization Summary

linking group Vi−L−Vi	link:cage	diffraction: *d* spacing [nm]
$-Me_2SiOSiMe_2-$	1:1	0.70, 0.37
	1.5:1	1.20, 0.72, 0.39
	2:1	1.05, 0.68, 0.39
$-Ph_2SiOSiPh_2-$	1:1	0.78, 0.39
$-(Me_2SiO)_7-$	1:1	0.74, 0.39
$-(Me_2SiO)_{10}-$	1:1	0.74, 0.39
	2:1	0.71, 0.38
$-(C_6H_4)-$	1:1	0.83, 0.38

alkyl trichloro or trialkoxy silanes or from sodium silicate precursors. This dramatic difference in the spectroscopic characterization of these materials versus that of traditional silicon resins implies that the traditional resins are not simply composed of cages linked together but contain many more silicon environments that are responsible for their correspondingly much more complicated NMR spectra. In looking at the wide-angle X-ray diffraction (WAXD) patterns of these small molecules and high-molecular-weight polymers, it is surprising how quickly these diffraction patterns become very broad, yielding very little definitive structural information. What we have seen is that the very pure smallest molecules prepared give sharp diffraction patterns. With more careful sample preparation, crystals suitable for single-crystal XRD analysis were obtained. The analysis on one material provides us definitive insights into a key building block of the higher molecular weight materials. The diffraction patterns of materials that are mixtures of 8−10 materials (as determined by APCI MS) now resemble what one typically sees for silicon resins. The interpretation of these broad diffraction patterns is not well understood.

While it is not clear to us if these polymers are indeed good models for the more common silicon resins, we have found that these materials can be well characterized by employing a variety of techniques. Through this characterization, we now know that polymeric or silicon resin materials that are simply composed of cages linked together yield relatively simple NMR spectra indicative of there being few chemical environments. Our work continues in studying the material properties of these relatively simple resin structures.

Acknowledgment. The GPC with triple-detection system studies were carried out by G. Gordon and E. Moyer, and their contributions are greatly appreciated. T. Michino is thanked for many helpful discussions on the synthesis of $^{H}T_8$ as well as supplying some of this material through the course of the study.

Supporting Information Available: Crystal structure and data refinement, atomic coordinates, bond lengths and angles, anistropic displacement parameters, and other relevent data for $C_8H_{26}O_{13}Si_{10}$. This material is available free of charge via the Internet at http://pubs.acs.org.

CM000325E